Volume XIII ● Issue 2/2022 ● Pages 99–115

INTERDISCIPLINARIA ARCHAEOLOGICA
NATURAL SCIENCES IN ARCHAEOLOGY

homepage: http://www.iansa.eu

Geochemical Study of Chert Artefacts from Xicotó Rockshelter (NE Iberia) Archaeological Site. New Data on Neolithic and Mesolithic Human Occupations

Marta Sánchez de la Torre[1*], Cynthia Belén González Olivares[1], Bernard Gratuze[2], François-Xavier Le Bourdonnec[3], Xavier Mangado[1]

[1]*SERP-IAUB. Universitat de Barcelona. 6–8 Montalegre St, 08001 Barcelona, Spain*
[2]*IRAMAT-CEB (UMR 5060). CNRS – Université d'Orléans. 3D Ferrollerie St, 45071 Orléans, France*
[3]*Archéosciences Bordeaux (UMR 6034). CNRS – Université Bordeaux Montaigne – Université de Bordeaux. Esplanade des Antilles, F-33607 Pessac Cedex, France*

A R T I C L E I N F O

Article history:
Received: 19th January 2022
Accepted: 4th August 2022

DOI: http://dx.doi.org/10.24916/iansa.2022.2.1

Key words:
lithic sourcing
human mobility
geochemistry
chert
Mesolithic
Neolithic
NE Iberia
Pre-Pyrenees

A B S T R A C T

Xicotó Rockshelter (Alòs de Balaguer, Lleida, Spain) is located in the eastern Pre-Pyrenean range in north-east Iberia, in the middle Segre River Basin. Since 2013, archaeological works have been developed by a team from the Prehistoric Studies and Research Seminar (SERP) at the University of Barcelona and up to three sedimentary levels have been identified. The preserved archaeological remains have allowed determining that the site was occupied during at least two different periods: the Ancient Neolithic and the Middle Mesolithic. The relative chronology given by the archaeological assemblage has been confirmed by several radiocarbon dates that place the occupations of the site to be during the VI and VII millennia cal BC. This paper presents the results obtained after the analysis of lithic raw materials from the entire lithic assemblage. The analysis was performed using the classic petroarchaeological approach, comprising textural and micropalaeontological descriptions, combined with the application of geochemical methods, using energy-dispersive X-ray fluorescence (ED-XRF) and laser-ablation inductively-coupled-plasma mass spectrometry (LA-ICP-MS). The results show that several rock types were selected for confectioning the lithic tools, among which chert was the preferred. Different types and origins have been identified, with similar sourcing strategies that involved local and regional procurement.

1. Introduction

The analysis of lithic raw materials provides essential information not only about the strategies involved in the procurement of the rocks used for the production of lithic assemblages of past human groups, but also on the territorial use of past communities. Studies of lithic raw materials were incorporated into archaeological research some decades ago as means of better understanding the behaviour of past human populations. In NE Iberia, such studies started during the 1990s and have increased in the first years of the 21st century. The classic approach to analyse lithic raw materials involved macroscopic characterisations to determine the textural and micropalaeontological content, as well as the use of petrographic analyses to determine mineralogical features (Mangado, 2005; Ortega, 2002; Terradas, 2001). However, the classic approach was limited in the case of sedimentary convergence facies, *i.e.* where two or more different geological formations possess similar characteristics and differences cannot be established (Aubry, 1990). In addition, the petrographic characterisation was a destructive tool, as a thin section was needed to perform the mineralogical description of the rock. With the aim of resolving these limitations and avoiding the use of destructive techniques, other methodological approaches have been tested in recent years (Roy-Sunyer *et al.*, 2013; Soto, 2015; Sánchez de la Torre, 2015). Following this trend, the use of geochemical tools to determine the origin of the archaeological chert

*Corresponding author. E-mail: martasanchezdelatorre@ub.edu

artefacts was incorporated a few years ago in NE Iberia with satisfactory results (Sánchez de la Torre *et al.*, 2017a; Sánchez de la Torre *et al.*, 2017c; Sánchez de la Torre *et al.*, 2019a).

This paper aims to present the archaeological site of Xicotó Rockshelter and its history of human occupation; the characterisation of the recovered lithic raw materials is used as means of tracing the mobility patterns and the territoriality of prehistoric people that occupied the site during the Ancient Neolithic and the Middle Mesolithic periods.

2. Materials and Methods

2.1 Xicotó Rockshelter: the site and the archaeological levels

The archaeological site of Xicotó Rockshelter (Alòs de Balaguer, Lleida, Spain) is located in the contact area between the Catalan Central Depression and the first Pre-Pyrenean Mountain Ranges. The site lies at 368 m asl and up to 100 m above the current Segre riverbed. The rock shelter possesses a maximum length of 18 m in its E-W axis and 8 m in the N-S axis. It was discovered in 1996 during a geoarchaeological survey in the Segre river basin (Bergadà *et al.*, 2007) and it is located 400 m to the east of the prehistoric site of Parco Cave (Mangado *et al.*, 2014). A survey to determine the archaeological potential of the site was undertaken in 1999. During these first investigations, 4 m^2 were excavated and resulted in several sedimentary levels possessing archaeological remains being identified. Within the archaeological evidence recovered, there were some faunal remains, pottery and lithic artefacts. In 2013, the archaeological work was restarted under the direction of two of us (Xavier Mangado and Marta Sánchez de la Torre) and still continues today.

As a first step, further 16 m^2 were opened, increasing the surface excavation to 24 m^2 in the following years (Figure 1).

Below a mixed level with evidence of human occupation during the Bronze Age, first sedimentary package of 40 cm was identified, with several hearths and pits. Recovered archaeological assemblage suggested relative chronology from the Ancient Neolithic (*e.g.* presence of impressed pottery and some *double bevel* geometric lithic tools) (Oms *et al.*, 2019), that was confirmed by a radiocarbon date from pit 1 (5300–5040 cal BC) (Figure 2). The second level was recognised below this first one, possessing mixed archaeological assemblage about 20 cm in width with a mixed set of materials moved from levels I and III. The sedimentary level III, which is still under excavation, possesses archaeological remains that can be exclusively related with a human occupation of the site during the Middle Mesolithic period (Figure 3). The large amount

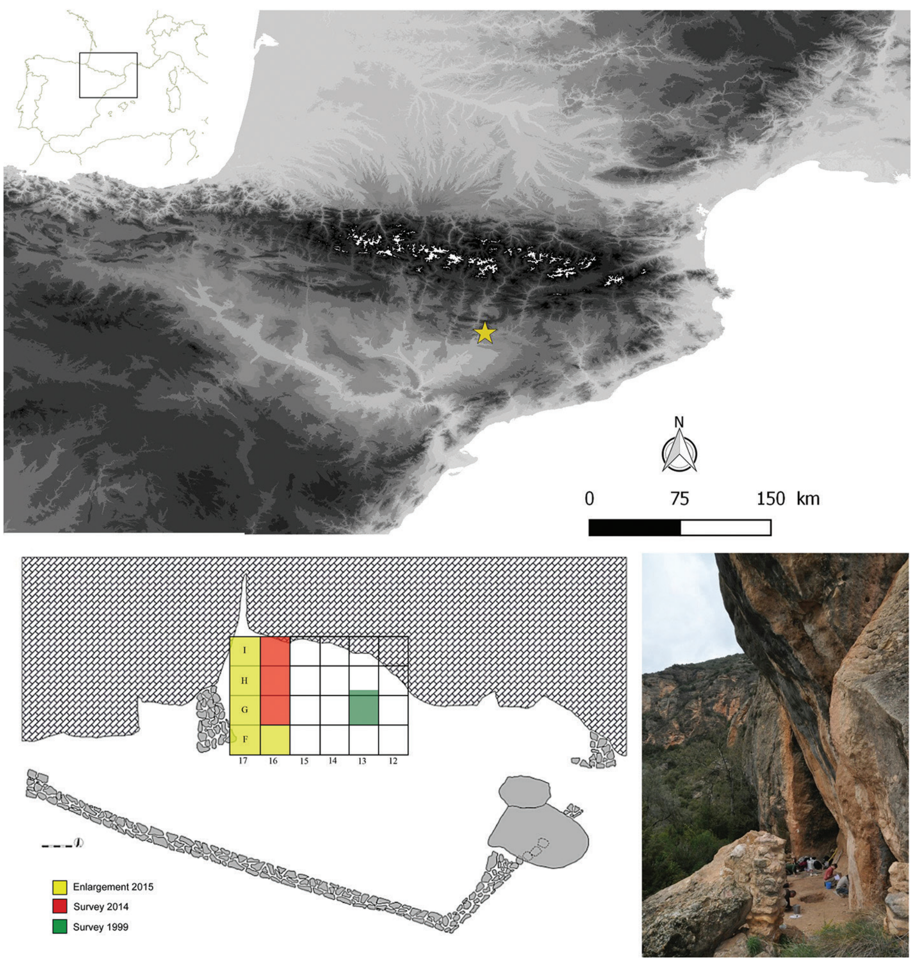

Figure 1. Xicotó Rockshelter location (top), archaeological grid (bottom left) and site detail area (bottom right).

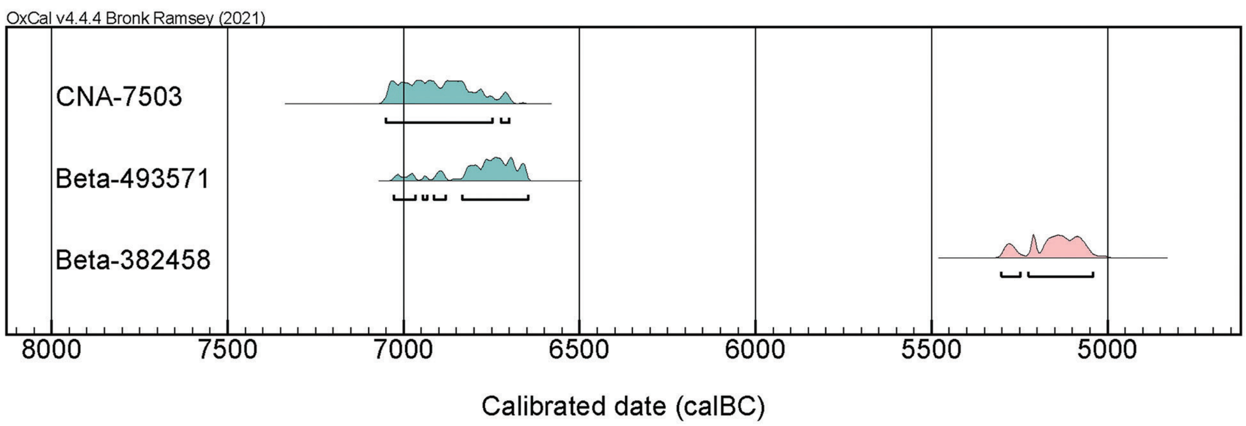

Lab code	Date BP	Material	Level
Beta-382458	6210±40 BP	Charcoal	I (Pit 1)
Beta-493571	7900±30 BP	Charcoal	III (Pit 12)
CNS-7503	7989±42 BP	Charcoal	III (Pit 12)

Figure 2. Representative lithic industry from levels I (top right) and III (top left) and radiocarbon dates and calibration after OxCal v.4.3.2 (Ramsey, 2017) with IntCal13 atmospheric curve (Reimer *et al.*, 2013) (bottom).

of notched and denticulated chert artefacts, as well as two radiocarbon dates from charcoals recovered at pit 12 (7050–6700 cal BP) (see Figure 2), allow us to set that the site was frequented during the Mesolithic facies known as Notch and Denticulates. This facies has been defined in the southern slopes of the Pyrenees by the dominance in the lithic industry of notched and denticulated tools (Alday, 2006).

2.2 Macroscopic and geochemical approaches

Firstly, a visual and micropalaeontological description of the entire lithic assemblage was undertaken (2383 samples). This macroscopic characterisation was carried out using a binocular microscope Olympus SZ61 (from 6.7 to 45 × magnification). Images were taken using a coupled Olympus SC30 camera. As the aim of the study was to analyse both

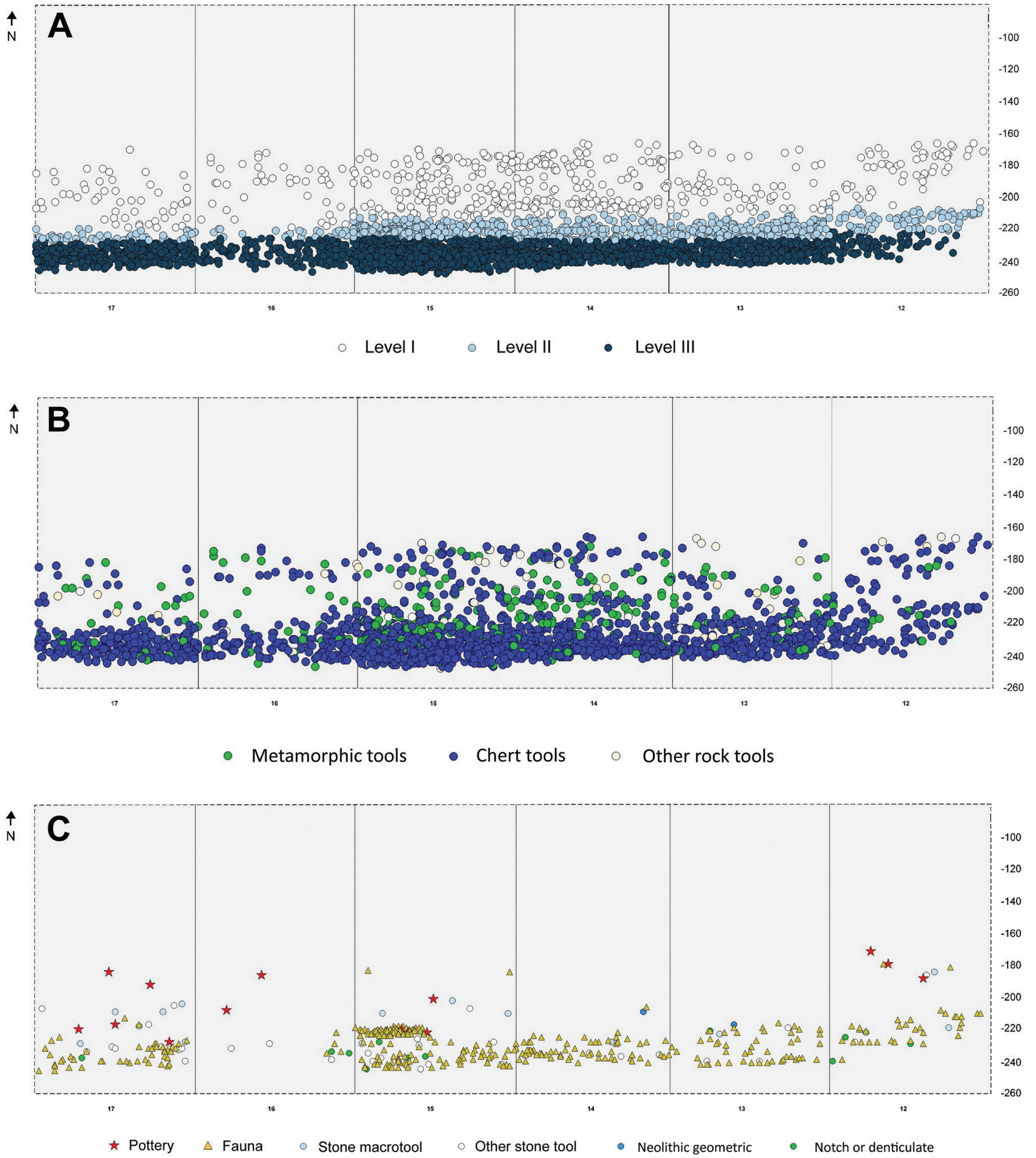

Figure 3. Materials dispersion with the three archaeological levels (A), the main types of rocks (B) and some representative archaeological remains (C).

geological and archaeological samples, non-destructive techniques were prioritised.

The second stage of this analytical approach involved geochemical analyses to quantify major, minor and trace components so as to be able to compare the raw materials of the chert artefacts with those from known geological outcrops. For this part of the study, 13 chert artefacts from level III of Xicotó Rockshelter were analysed by energy-dispersive X-ray fluorescence (ED-XRF) and 36 artefacts (also from the same level) were studied with laser-ablation inductively-coupled-plasma mass spectrometry (LA-ICP-MS). Archaeological tools without cortex and surface alterations were preferred.

With the aim of comparing results obtained after the analysis of archaeological samples, geological formations with cherts having similar characteristics to those of the

Table 1. Outcrops and archaeological samples selected for study with the number of samples analysed by each geochemical method.

ACRONYM	OUTCROP / SITE	FORMATION	AGE	TYPE	ED-XRF	LA-ICP-MS
ALB1	Alberola 1	Tartareu-Alberola	Oligocene	Lacustrine	20	20
ALB2	Alberola 2	Tartareu-Alberola	Oligocene	Lacustrine	16	17
CDF	Castelló de Farfanya	Castelltallat Fm	Oligocene	Lacustrine	51	49
PC	Puente Candasnos	Aragonian limestones	Miocene	Lacustrine	23	20
PERAL	Peraltilla	Castelltallat Fm	Oligocene	Lacustrine	23	20
ZURI	Zurita	Tremp Fm (2)	Maastrichtian	Lacustrine	18	13
FONT	Fontllonga	Tremp Fm (1)	Maastrichtian	Evaporitic	–	19
ALI	Alins del Monte	Tremp Fm (1)	Maastrichtian	Evaporitic	–	30
CER	Cérizols	Bleu tertiary	Danian	Evaporitic	–	17
VSSM	Vessant Sud Sant Mamet	Tremp Fm (1)	Maastrichtian	Evaporitic	–	21
MONTG	Montgaillard	Flysch limestones	Turonian-Santonian	Marine	–	20
MONTS	Montsaunès	Nankin Fm	Maastrichtian	Marine	–	20
BUALA	Buala	Marly flysch	Campanian-Maastrichtian	Marine	–	20
XICOTÓ	Xicotó Rockshelter	–	–	Lacustrine	13	17
XICOTÓ	Xicotó Rockshelter	–	–	Evaporitic	–	17
XICOTÓ	Xicotó Rockshelter	–	–	Marine	–	2

artefacts from Xicotó were surveyed and sampled. It involved up to 13 outcrops from 9 geological formations, with more than 160 samples being selected for geochemical analyses (Table 1). Only primary outcrops were considered for this study. To improve analysis time and to avoid surface alterations, geological samples were prepared in squares of 5 × 5 mm, removing cortex surfaces.

To analyse major and minor elements, energy-dispersive X-ray Fluorescence (ED-XRF) was employed. Analyses were done at the Archéosciences-Bordeaux Laboratory, Pessac, France. Nine element concentrations were quantified (Na, Mg, Al, Si, P, K, Ca, Ti, Fe) using an X-ray fluorescence spectrometer SEIKO SEA 6000 VX (Orange *et al.*, 2017), using fundamental parameters corrected by the granodiorite GSP2 from the US Geological Survey (USGS) international standard (Wilson, 1998). A 3×3 mm collimator was prioritised, and analysis time was set to 400 s for each measurement condition (3 conditions with air or He environment and Cr or Pb filter were established). To check instrument calibration and accuracy, the JCh-1 chert standard from the Geological Survey of Japan (GSJ) was employed (Imai *et al.*, 1996). To prove and validate the formula which was used and to check instrument accuracy, a measurement with the JCh-1 chert standard was established, with the standard deviation obtained always being lower than 0.08 w%, validating the accuracy of the formula used (Sánchez de la Torre *et al.*, 2017b).

To analyse trace elements, we used laser-ablation inductively-coupled-plasma mass spectrometry (LA-ICP-MS) at the Ernest Babelon Laboratory, IRAMAT, Orleans, France. Elements were quantified using a Thermo Fisher Scientific Element XR mass spectrometer associated with a Resonetics RESOlution M50e ablation device. This spectrometer has the advantage of being equipped with a dual mode (counting and analogue modes) secondary electron multiplier (SEM) with a linear dynamic range of over nine orders of magnitude, associated with a single Faraday collector which allows an increase in the linear dynamic range by additional three orders of magnitude. This feature is particularly important for laser-ablation analysis of lithic samples, as it is possible to analyse major, minor and trace elements in a single run regardless of their concentrations and their isotopic abundance. The ablation device is an excimer laser (ArF, 193 nm), which was operated at 7–8 mJ and 20 Hz and only if saturation was observed were conditions reduced to 10 Hz. A dual gas system with helium (0.65 l/min) released at the base of the chamber, and argon at the head of the chamber (1.1 l/min) carried the ablated material to the plasma torch. Ablation time was set to 40 s: 10 s pre-ablation to let the ablated material reach the μμspectrometer and 30 s collection time. Laser spot size was set to 100 μm, and only reduced to 80 or 50 μm if saturation was detected, and line mode acquisition was chosen to enhance sensitivity. Background measurements were run every 10–20 samples. Fresh fractures were analysed on geological samples to reduce potential contamination. Priority was given to characterising large samples; thus, only one ablation line was carried out per specimen. However, if element spikes due to the presence of inclusions or heterogeneities were observed during analysis, results were discarded and a new ablation location was selected.

Calibration was performed using a standard reference glass NIST610 which was run periodically (every 10–20 samples) to correct for drift. NIST610 was used to calculate the response coefficient (k) of each element (Gratuze, 1999; Gratuze, 2014), and the measured values of each element

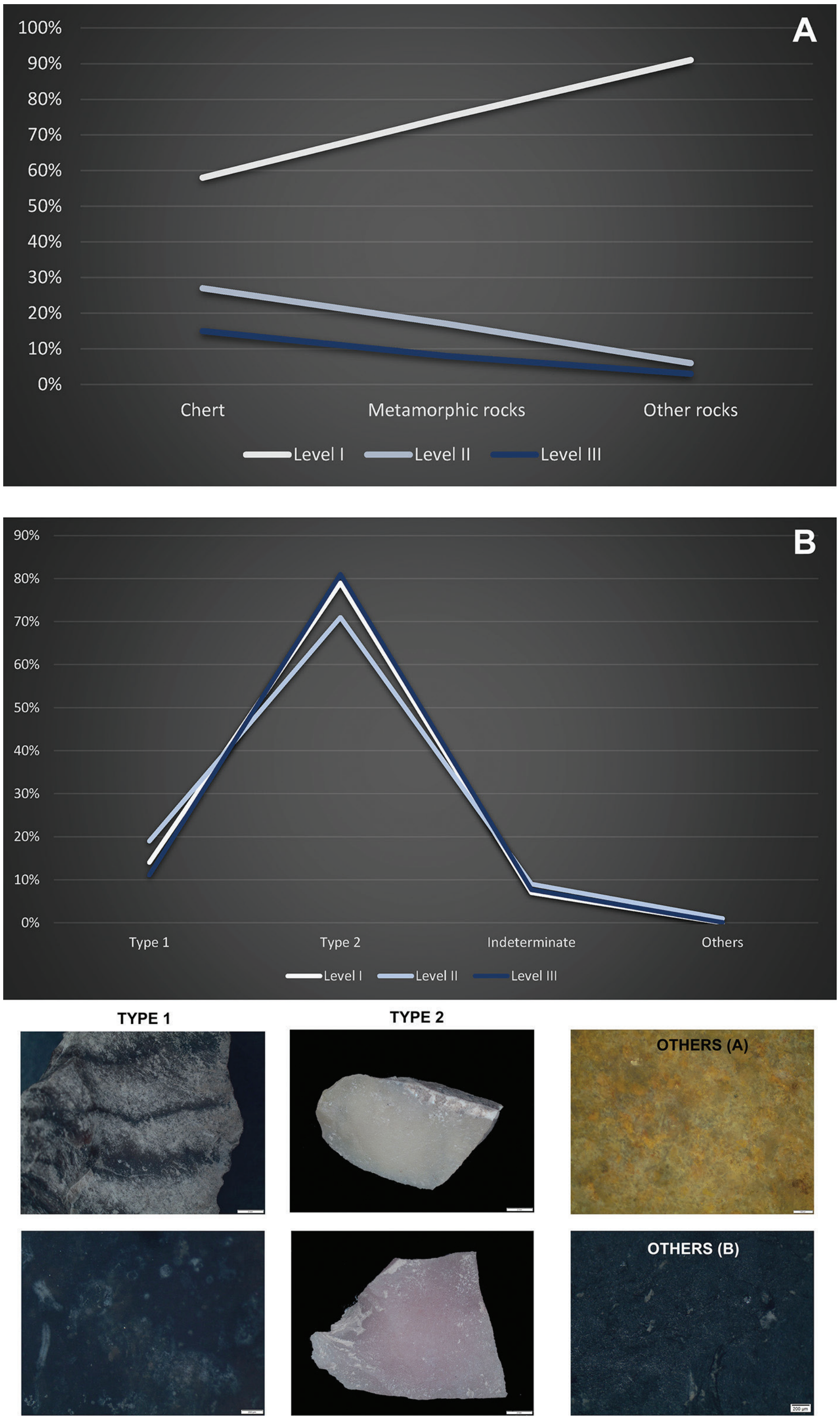

Figure 4. Main lithological groups from the lithic industry by levels (A), chert types by levels (B) and macroscopic views of the different groups (bottom).

were normalised against 28Si, the internal standard, to produce a final percentage. Glass Standard NIST612 was analysed independently of calibration to provide comparative data. In all, 30 elements were quantified (Li, Be, B, Mg, Al, Si, Ca, Ti, V, Cr, Fe, Ga, Ge, As, Rb, Sr, Y, Zr, Nb, Cs, Ba, La, Ce, Pr Nd, Sm, W, Bi, Th and U).

3. Results

3.1 Macroscopic characterisations: chert types and related formations

From the 2383 lithic artefacts that were recovered from the three sedimentary levels from Xicotó, 1958 were made of chert (82%). Fine-grain metamorphic rocks defined as hornfelses made up 12% of the assemblage, the remaining being 6% other metamorphic and igneous rocks like quartzites and granites. In Level I, the Ancient Neolithic occupation, chert represented 58% of the set, the rest largely represented by hornfelses and other rocks (27% and 15%). However, in the Middle Mesolithic occupation from level III, the presence of chert increased up to 91%, the other rocks being anecdotic (quartzites 6% and other rocks 3%) (Figure 4 A). This significant difference between levels with regard to the lithology is probably related to changes in the typology of the retouched lithic assemblage. Thus, hornfelses and other metamorphic and igneous rocks are mostly related with the manufacture of macrotools, whereas chert is mostly used for confectioning carving artefacts obtained from flakes by direct percussion. Accordingly, during the Ancient Neolithic, the production of macrotools is predominant in the archaeological set (39% of the finished tools). By contrast, in the Middle Mesolithic, the macrotools were reduced to 10%, whereas other typological tools like notches and denticulates increased (42% of the finished tools). These tools possess extensive discontinued deep retouches frequently inverse or alternate with generally a significant presence of cortical surfaces. The macroscopic observation of the archaeological cherts has allowed us to determine two main types (1 and 2) and some evidence of other types (A and B), the latter only being represented by some scarce elements (2 pieces from type A and 1 from type B), suggesting that these raw materials were only occasionally procured. The presence of each chert type by levels is quite homogeneous, type 2 being the most represented in the three sedimentary levels (Figure 4 B).

Type 1 is represented by 253 artefacts, which means 13% of the set. The distribution of this chert type by levels is quite homogeneous, representing 14% in level I and 11% in level III. Macroscopically this chert has a heterogeneous texture with metal oxides, micritic residues, grains of detrital quartz and probably organic matter inclusions. The main micropalaeontological content consists of sections of *Charophyte algae* and some gastropods. These cherts originated in a lacustrine sedimentary environment, with parallels in four different geological formations. A description of the main features of each formation, follows. More detailed descriptions can be found in Sánchez de la Torre *et al.* (2017c).

- The **Tremp formation** (2) (Maastrichtian, Upper Cretaceous) possesses a level of laminated micritic limestones with *Charophyte algae* and gastropod moulds filled with sparite (IGME, e.p.). This formation contains nodular cherts and outcrops in the Carrodilla Mountain Range, a Pre-Pyrenean foothill located between the Cinca River Basin to the west and the Noguera Ribagorzana River to the east (Zurita outcrop, ZURI). Cherts have a texture with impurities of mineral oxides, carbonate residues and probably organic matter. The main micropalaeontological content is composed of *Charophyte algae* and gastropods.
- The **Castelltallat formation** (Rupelian, Oligocene) largely outcrops in Serra Llarga (IGME, 1998), a mountain range located in the province of Lleida, in the contact area between the Pre-Pyrenees and the Central Depression. Nodular cherts appear within the stratified limestone, more than 40 primary outcrops having been identified along the Serra Llarga some years ago (Castelló de Farfanya outcrops, CDF) (Mangado, 2005). The presence of chert nodules from this formation has also been noticed several kilometres to the west of Serra Llarga and close to the Cinca River (Peraltilla outcrop, PERAL) (Sáez, 1987). Cherts from this formation have a macroscopic texture with metal oxides, carbonate remains, detrital quartz and probable organic matter. *Charophyte algae* and lacustrine gastropods constitute the main micropalaeontological content.
- The **Tartareu-Alberola** cherts (Rupelian, Oligocene) appear within the lacustrine stratified limestones outcropping in the Sant Miquel Mountain Range, a Pre-Pyrenean Mountain Chain located to the north of Serra Llarga and limited by the Noguera Ribagorzana River to the west and the Farfanya River to the east. Two primary outcrops were identified during the surveys (Alberola 1outcrop, ALB1 and Alberola 2 outcrop, ALB2). This chert type has macroscopic heterogeneous textures with metal oxides and abundant micritic remains. The micropalaeontological content is formed of *Charophyte algae* and gastropod sections.
- The **Aragonian limestone formations** containing chert nodules (Aquitanian-Vindobondian, Miocene) outcrops in the Central Depression of the Middle Ebro Basin (Puente Candasnos outcrop, PC) (IGME, *e.p.*). This chert has homogeneous textures with metal oxides, carbonate remains, probable organic matter and some detrital quartz crystals. *Charophyte algae* and gastropod sections make up the micropalaeontological content.

Type 2 is formed by 1550 elements, being the most represented chert type (79% of the set), being similar the distribution by levels (79% in the Ancient Neolithic and 81% in the Middle Mesolithic). This raw material is characterised by the absence of bioclastic content, as it originated in a hypersaline sedimentary environment. The textures are quite smooth, with only a few inclusions of metal oxides and lenticular gypsum pseudomorphs. Parallels can be macroscopically drawn with cherts from the Tremp formation, outcropping largely in the central and eastern southern Pyrenees and the blue cherts from the Danian outcropping in the northern slopes of the Pyrenees.

The **Tremp formation** (1) largely outcrops in the southern slopes of the central and eastern Pre-Pyrenees. Cherts are embedded within the lacustrine limestones from the Garumnian facies of this formation (IGME, 2006). Chert outcrops have been located in the Carrodilla Mountain Range (Alins del Monte outcrop, ALI) and the Montsec

Mountain Range, with several outcrops being defined, from which two have been selected for this study (Fontllonga outcrop, FONT and Vessant Sud de Sant Mamet outcrop, VSSM). Cherts possess a homogeneous texture with some metal inclusions, the main feature of this chert type being the absence of micropalaeontological content. In some cases, lenticular gypsum crystals are identified.

The **Tertiary *bleu* cherts** (Danian, Paleocene) are recognised within the limestone formations from the Danian outcropping in the *Petites-Pyrénées* and the Plantaurel regions, as well as in the Aurignac massif, in the northern slopes of the Pyrenean Mountain Chain (Simonnet, 1999) (outcrop selected for analysis: Cérizols, CER). These cherts have homogeneous textures without bioclastic content, the sole inclusion being some metal oxides.

Besides the two main types, other textures were identified. The first one (**type A**) is only represented by two specimens, both found in the Middle Mesolithic level. Macroscopically, both samples are characterised by a heterogeneous texture composed of abundant metal oxides and detrital quartz crystals, the main micropalaeontological content being composed of sponge spicules. This chert type is macroscopically similar with the two chert sources outcropping in the northern slopes of the Central Pyrenees: The Montgaillard flysch cherts from the Turonian-Santonian and the Montsaunès-Buala cherts from the Nankin formation (Maastrichtian). A summary with the main features of each formation follows. More detailed descriptions can be found in Sánchez de la Torre *et al.* (2019b).

The Turonian-Santonian cherts from the **Montgaillard** outcrop (MONTG) originate in the flysch limestones outcropping primarily in the Dussert quarry, near Montgaillard town, in the northern central Pyrenees (Barragué *et al.*, 2001). These cherts are macroscopically composed of a heterogeneous texture with metal oxides and detrital quartz crystals. The micropalaeontological content is formed of sponge spicules and some small benthic foraminifera.

The Campanian-Maastrichtian flysch cherts come from the Buala outcrop (BUALA) outcrop in the old Buala quarry, near Montgaillard town, in the northern central Pyrenees. These cherts present a heterogeneous texture with metal oxides, detrital quartz cristals, sponge spicules, some small pelagic foraminifera and, in some cases, probable siderolites.

The Maastrichtian cherts from the Nankin Formation (Montsaunès outcrop) (MONTS) are inserted in the Nankin formation limestones, outcropping in the northern slope of the central Pyrenees, near the ancient quarry of Montsaunès (Montsaunès outcrop, MONTS). These cherts possess a heterogeneous texture with carbonate relicts, detrital quartz and metal oxides. The micropalaeontological content is composed of sponge spicules and some small foraminifera.

The second texture was defined as **type B** and represented by only a single specimen, found in the transitional level (level II). Macroscopically it consists of inclusions of abundant quartz crystals and calcite or dolomite rhombohedral crystals, and sponge spicules and small foraminifera as the main micropalaeontological content. This specimen can directly be related to cherts from the Agua-Salenz formation (Conacian), outcropping in the southern slopes of the Central Pyrenees, near the Turbón Massif. However, considering that this artefact is attributed to the transitional level, we will not particularly take it into account during the later discussion.

3.2 Geochemical characterisations: connecting archaeological cherts with specific outcrops

To try to establish a connection between the different chert types identified in the archaeological record and specific chert outcrops, geochemical methods were employed. The 13 lacustrine chert artefacts from level III were analysed by ED-XRF to determine major and minor components and were compared with 151 samples from six chert outcrops from four geological formations. Only lacustrine samples were studied using this geochemical approach, as previous studies revealed that this technique was not discriminant when analysing other types of chert (Sánchez de la Torre *et al.*, 2017b). While nine oxides were measured within ED-XRF (Na_2O, MgO, Al_2O_3, SiO_2, P_2O_5, K_2O, CaO, TiO_2 and Fe_2O_3), data relating to Na_2O and P_2O_5 was limited as their values were frequently below the equipment's detection limits. Median values and the standard deviation for each geological outcrop and the values for all the archaeological samples in w% are presented in Table 2.

The lacustrine cherts recovered at Xicotó possess similar macroscopic features to the cherts outcropping in the Tartareu-Alberola unit, the Castelltallat formation, the Tremp formation (2) and the Aragonian limestones, and with outcrops from 25 to 100 km from the site. The scatterplot concerning three of the main components (Fe_2O_3, Al_2O_3 and SiO_2) (Figure 5, top) shows that some differences can be observed between the different geological sources. However, there is an overlapping area, so results cannot be taken to be conclusive. Nevertheless, several formations could be already discarded: the Tartareu-Alberola cherts (Alberola 1 and Alberola 2) as well as the Aragonian cherts (Puente Candasnos) seem to be far from the main dispersion of the archaeological samples. In a similar way, the main groups from the Maastrichtian cherts (Zurita outcrop) and the Peraltilla outcrop from the Castelltallat formation do not fit with the samples from Xicotó. Thus, the lacustrine cherts from Xicotó seem to better fit with cherts from the Castelló de Farfanya outcrop (Castelltallat formation).

As the ED-XRF results were not conclusive for the lacustrine cherts and the other chert types had not yet been studied, we also developed LA-ICP-MS analyses to quantify the trace elements. Thus 17 lacustrine chert artefacts, 17 evaporitic chert tools and the two recognised marine cherts from level III were analysed by LA-ICP-MS to specifically determine trace elements and were compared with up to 286 samples from 13 chert outcrops from nine geological formations. Up to 30 elements were quantified using this method (Li, Be, B, Mg, Al, Si, Ca, Ti, V, Cr, Fe, Ga, Ge, As, Rb, Sr, Y, Zr, Nb, Cs, Ba, La, Ce, Pr, Nd, Sm, W, Bi, Th and U). Median values and the standard deviation for each geological outcrop and the values for all the

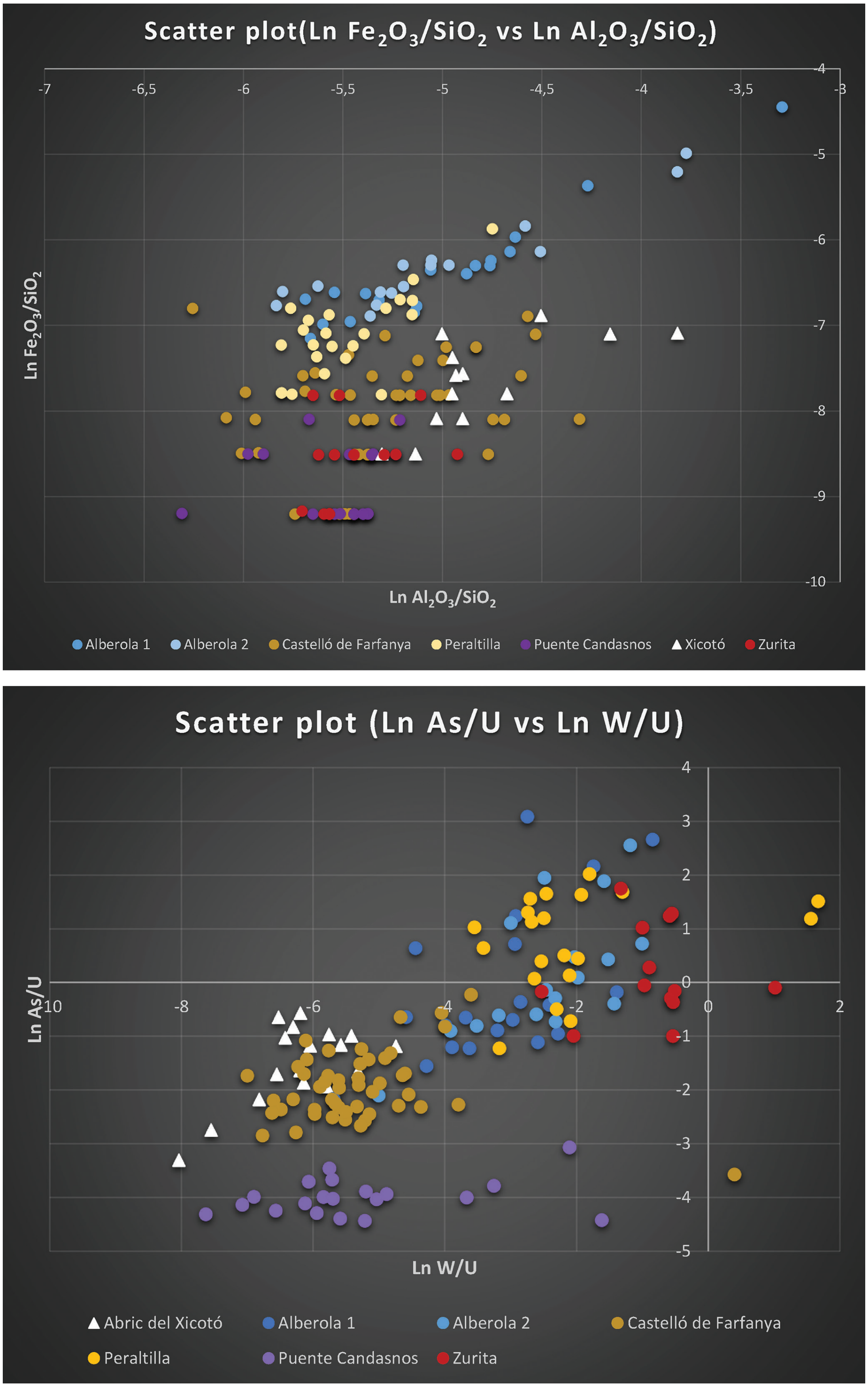

Figure 5. Scatterplot for Ln As/W vs Ln W/U representing all the lacustrine geological outcrops (circles) and the lacustrine archaeological samples of Xicotó (triangle).

Table 2. Median values and standard deviations (in brackets) for each geological outcrop and values for each archaeological sample with the nine elements quantified by ED-XRF in w%.

Variable	Al_2O_3	CaO	Fe_2O_3	K_2O	MgO	Na_2O	P_2O_5	SiO_2	TiO_2
ALB1	1.02 (1.22)	3.02 (2.92)	0.27 (0.37)	0.16 (0.24)	0.31 (0.21)	<LOD	<LOD	95.44 (3.22)	0.04 (0.06)
ALB2	0.75 (0.56)	2.88 (2.27)	0.21 (0.15)	0.12 (0.08)	0.44 (0.24)	<LOD	<LOD	95.92 (2.47)	0.03 (0.03)
CDF	0.61 (0.55)	2.17 (10.62)	0.10 (0.43)	0.03 (0.02)	0.31 (0.22)	<LOD	<LOD	97.07 (11.24)	0.02 (0.04)
PERAL	0.42 (0.13)	2.75 (1.58)	0.09 (0.05)	0.05 (0.02)	<LOD	<LOD	<LOD	96.68 (1.55)	0.02 (0.01)
PC	0.41 (0.09)	0.28 (0.38)	0.02 (0.01)	0.02 (0.01)	0.08 (0.01)	<LOD	<LOD	99.30 (0.36)	0.01 (0.00)
ZURI	0.43 (0.10)	0.28 (0.81)	0.02 (0.01)	0.02 (0.01)	<LOD	<LOD	<LOD	99.25 (0.79)	<LOD
Xicotó-05	0.64	0.58	0.03	0.17	0.66	<LOD	0.13	97.79	0.01
Xicotó-07	0.71	0.28	0.05	0.09	0.38	<LOD	0.04	98.44	0.01
Xicotó-08	0.72	2.32	0.05	0.09	0.32	<LOD	0.13	96.35	0.01
Xicotó-09	0.73	0.37	0.03	0.16	0.45	<LOD	0.37	97.89	<LOD
Xicotó-10	1.52	0.33	0.08	0.25	0.6	<LOD	0.21	96.98	0.02
Xicotó-11	0.65	1.98	0.08	0.09	0.38	<LOD	0.16	96.64	0.02
Xicotó-14	0.68	2.93	0.06	0.03	0.28	<LOD	0.08	95.94	0.02
Xicotó-18	1.08	0.39	0.1	0.14	0.58	<LOD	0.09	97.61	<LOD
Xicotó-19	0.69	1.09	0.04	0.1	0.46	<LOD	0.11	97.51	0.01
Xicotó-22	0.49	0.46	0.02	0.06	0.28	<LOD	0.12	98.56	<LOD
Xicotó-23	0.91	0.75	0.04	0.14	0.49	<LOD	0.12	97.55	0.01
Xicotó-24	0.58	0.71	0.02	0.07	0.03	<LOD	0.03	98.56	<LOD
Xicotó-26	2.11	0.76	0.08	0.26	0.77	<LOD	<LOD	95.99	0.03

archaeological samples in ppm% are presented in Table 3. According to the LA-ICP-MS results, some trace elements could be relevant for distinguishing between sources. Regarding the lacustrine cherts, the values for As, W and U clearly separate the different geological sources, being in this case the archaeological samples from Xicotó directly related to cherts from the Castelló de Farfanya outcrop (Figure 5, bottom).

The evaporitic chert artefacts from Xicotó Rockshelter were macroscopically similar to the southern Pre-Pyrenean cherts from the Garumnian facies of the Tremp Formation (Alins del Monte, Fontllonga and Vessant Sud de Sant Mamet outcrops) and the northern Pre-Pyrenean *bleu* cherts from the Danian (Cérizols outcrop). A discriminant analysis (DA) was run using XLSTAT software (Addinsoft, 2020) to see if quantified distinctions were visible at the minor elemental levels. The DA of the four geological outcrops and the archaeological samples of Xicotó concerning three specific trace elements (Be, B and U values) showed that some differences can indeed be immediately observed between formations. Of the 98.36% of the total variance F1 (77.69%) and F2 (20.67%) is represented. Both in the presentation of all the samples (Figure 6, top) and only the centroids (Figure 6, bottom) it can be highlighted that cherts outcropping in the northern Pyrenees (Cérizols outcrop) do not fit with the main dispersion (cluster) of the archaeological samples. The large number of samples from Xicotó can mostly be related to cherts from Vessant Sud de Sant Mamet outcrop, according to the geochemical analysis of specific trace elements.

Finally, the two chert artefacts found in level III with macroscopic textures associated to marine cherts were studied by LA-ICP-MS and compared with geological samples from the flysch cherts from Montgaillard and cherts from the Nankin formation (Buala and Montsaunès outcrops), all of them outcropping in the northern Pyrenees. The scatterplot concerning specific trace elements (Ti, Sr and Th) (Figure 7) clearly separates the three outcrops, the archaeological samples being placed in the dispersion area of the Montgaillard group.

4. Discussion

The macroscopic analysis of the lithological assemblage recovered at the Xicotó Rockshelter site has revealed that the nature of the rocks was adapted to the functionality of the artefacts. Thus, during the Ancient Neolithic period, metamorphic and igneous rocks such as hornfelses and granites were largely exploited for manufacturing macrotools, for example, hand mills, mortars and grinding stones. However, during the Middle Mesolithic period, the presence of these rocks significantly decreased. Unfortunately, the origin of the hornfelses and other metamorphic and igneous rocks has not yet been established. However, near to the site in the Segre riverbed these rocks are nowadays abundant.

Regarding the origin of chert artefacts, type 2, which is the most abundant chert type found in the two human occupations, seems to be directly related to cherts from the

Table 3. Median values and standard deviations (in brackets) for each geological outcrop with the nine elements quantified by LA-ICP-MS in ppm. Data from archaeological samples can be found in the Supplementary Raw Data file.

Variable	Li	Be	B	Mg	Al	Si	Ca	Ti	V	Cr	Fe	Ga	Ge	As
ALB1	20.67 (9.82)	0.51 (0.29)	41.97 (26.14)	2570.92 (1205.97)	9712.97 (8937.50)	406164.10 (46288.87)	71674.31 (74266.16)	519.14 (423.77)	19.39 (16.60)	13.44 (8.63)	4522.34 (3901.88)	28.72 (39.21)	0.49 (0.12)	11.22 (13.03)
ALB2	18.76 (8.90)	0.40 (0.2)	39.49 (12.37)	2819.19 (1157.20)	7721.62 (4609.65)	417378.93 (26698.20)	58012.88 (44655.41)	504.68 (348.99)	14.39 (8.38)	11.42 (5.56)	3500.53 (1826.71)	24.59 (16.99)	0.52 (0.14)	4.01 (3.29)
ALI	0.88 (1.24)	0.33 (0.13)	25.82 (9.96)	84.39 (184.46)	269.44 (761.81)	465558.38 (1807.01)	1831.27 (1038.42)	51.90 (40.30)	4.26 (13.67)	2.35 (1.60)	335.67 (602.47)	22.29 (102.09)	<LOD	2.38 (2.63)
BUALA	18.31 (6.17)	0.13 (0.09)	110.23 (8.86)	72.54 (49.32)	1071.67 (874.76)	460541.83 (4220.74)	1970.71 (681.84)	125.31 (110.66)	7.05 (5.43)	22.75 (12.41)	6379.06 (5526.08)	7.36 (8.64)	0.60 (0.22)	8.91 (8.32)
CDF	13.27 (7.31)	0.17 (0.10)	56.50 (12.09)	540.92 (549.82)	2193.91 (2251.09)	450758.81 (23874.27)	20067.27 (36294.54)	169.79 (316.46)	4.67 (5.06)	4.69 (3.06)	1275.34 (1612.18)	12.97 (9.40)	0.48 (0.14)	8.26 (5.31)
CER	4.61 (4.50)	0.10 (0.05)	51.82 (35.29)	36.75 (17.33)	86.57 (57.56)	465523.30 (812.80)	2224.10 (1088.48)	48.64 (20.76)	1.47 (0.86)	2.63 (1.06)	423.16 (357.49)	2.09 (2.98)	<LOD	1.77 (1.42)
FONT	0.51 (0.50)	0.12 (0.07)	15.23 (15.26)	53.27 (85.14)	150.58 (378.11)	464611.60 (4537.01)	3874.76 (6705.12)	34.79 (35.11)	0.39 (0.63)	2.05 (1.45)	92.28 (164.39)	1.18 (1.16)	<LOD	1.30 (0.95)
MONTG	12.11 (7.13)	0.06 (0.05)	64.20 (19.49)	170.75 (201.75)	2265.64 (3007.38)	463293.49 (3830.70)	4537.03 (5195.78)	165.10 (91.51)	6.21 (8.41)	13.32 (10.56)	3549.10 (5357.62)	5.58 (2.69)	0.66 (0.19)	5.15 (7.82)
MONTS	9.90 (4.15)	0.14 (0.05)	111.15 (22.63)	93.73 (47.67)	1355.81 (698.73)	464669.27 (1681.56)	2623.20 (991.31)	222.65 (145.78)	9.99 (6.99)	15.95 (9.55)	2348.13 (2110.58)	3.44 (1.21)	0.24 (0.06)	7.79 (6.76)
PERAL	15.46 (5.67)	0.16 (0.07)	62.91 (9.51)	1346.62 (899.27)	3299.64 (1920.55)	421340.51 (34133.46)	61376.29 (51978.68)	246.92 (170.46)	8.45 (9.76)	7.49 (3.46)	2008.55 (891.10)	32.84 (19.50)	0.50 (0.36)	12.50 (9.48)
PC	7.13 (4.97)	0.23 (0.06)	43.78 (6.91)	173.01 (110.29)	964.58 (617.38)	461255.85 (5484.60)	7145.75 (7511.34)	153.24 (114.02)	2.33 (1.43)	4.65 (3.46)	371.80 (186.27)	2.75 (2.71)	0.36 (0.05)	2.10 (0.66)
VSSM	4.98 (6.67)	0.23 (0.20)	13.45 (12.67)	53.75 (91.50)	107.10 (143.79)	463422.66 (10089.95)	5340.28 (15386.86)	44.34 (32.81)	3.24 (10.65)	2.56 (1.11)	480.36 (772.90)	1.98 (1.20)	0.61 (0.14)	2.15 (2.57)
ZURI	2.53 (1.90)	0.10 (0.09)	37.62 (32.48)	254.65 (253.93)	483.61 (598.21)	457359.04 (15665.83)	13475.12 (23505.41)	96.67 (56.46)	3.24 (3.98)	4.19 (2.05)	708.36 (875.59)	3.59 (1.86)	<LOD	4.48 (4.41)

Table 3. Median values and standard deviations (in brackets) for each geological outcrop with the nine elements quantified by LA-ICP-MS in ppm. Data from archaeological samples can be found in the Supplementary Raw Data file. (*Continuation*)

Variable	Rb	Sr	Y	Zr	Nb	Cs	Ba	La	Ce	Pr	Nd	Sm	W	Bi	Th	U
ALB1	16.61 (14.54)	293.41 (337.69)	1.32 (1.00)	10.62 (15.76)	1.58 (1.28	1.04 (0.97)	138.56 (224.35)	3.82 (5.27)	7.66 (10.59)	0.78 (0.97)	2.92 (3.45)	0.50 (0.43)	0.40 (0.26)	0.14 (0.12)	1.42 (1.39)	11.14 (9.07)
ALB2	13.67 (8.61)	326.29 (266.04)	2.17 (2.95)	8.81 (13.44)	1.48 (0.91)	0.87 (0.58)	117.61 (119.24)	2.70 (2.53)	5.88 (6.79)	0.61 (0.57)	2.37 (2.32)	0.50 (0.54)	0.26 (0.13)	0.09 (0.05)	1.21 (1.17)	4.43 (5.11)
ALI	0.66 (1.53)	7.82 (21.17)	0.07 (0.14)	0.34 (0.66)	0.19 (0.36)	0.07 (0.13)	100.54 (473.07)	0.12 (0.28)	0.74 (2.34)	0.06 (0.12)	0.12 (0.24)	0.04 (0.06)	4.45 (6.79)	0.24 (0.19)	0.05 (0.11)	58.20 (22.56)
BUALA	1.30 (0.97)	13.51 (8.12)	0.77 (0.60)	4.19 (1.62)	0.41 (0.22)	0.09 (0.09)	30.06 (43.72)	0.74 (0.49)	1.65 (1.07)	0.23 (0.15)	0.85 (0.58)	0.22 (0.15)	3.58 (8.55)	0.16 (0.07)	1.30 (0.58)	0.67 (0.17)
CDF	3.40 (4.19)	61.91 (98.82)	0.47 (0.55)	2.75 (7.24)	0.48 (0.74)	0.20 (0.30)	57.07 (48.73)	0.61 (0.99)	1.31 (1.97)	0.15 (0.22)	0.52 (0.69)	0.13 (0.17)	0.57 (2.27)	0.11 (0.12)	0.35 (0.46)	54.04 (28.65)
CER	0.35 (0.17)	2.09 (1.24)	0.11 (0.10)	0.30 (0.21)	0.17 (0.22)	0.06 (0.06)	8.36 (10.46)	0.13 (0.09)	0.38 (0.38)	0.08 (0.07)	0.16 (0.12)	0.06 (0.07)	4.32 (6.09)	0.31 (0.37)	0.05 (9.03)	2.97 (2.91)
FONT	0.31 (0.56)	3.66 (8.24)	0.06 (0.07)	0.15 (0.18)	0.07 (0.10)	0.07 (0.08)	3.61 (3.83)	0.05 (0.08)	0.12 (0.21)	0.03 (0.03)	0.04 (0.05)	0.03 (0.03)	3.31 (7.91)	0.90 (2.31)	0.04 (0.04)	2.69 (2.73)
MONTG	3.65 (5.01)	34.91 (61.98)	1.51 (2.26)	2.29 (1.69)	0.43 (0.32)	0.25 (0.37)	51.20 (66.92)	1.26 (1.46)	2.54 (3.70)	0.30 (0.34)	1.26 (1.53)	0.30 (0.37)	1.04 (1.41)	0.26 (0.32)	0.46 (0.38)	0.25 (0.06)
MONTS	3.10 (1.92)	7.74 (9.12)	0.97 (1.51)	4.10 (9.13)	0.62 (0.53)	0.25 (0.16)	15.70 (8.75)	2.19 (3.81)	2.31 (2.12)	0.51 (0.76)	1.86 (2.80)	0.34 (0.50)	1.13 (0.62)	0.21 (0.16)	0.74 (0.36)	1.02 (0.43)
PERAL	6.00 (5.83)	399.93 (339.97)	0.58 (0.32)	2.87 (2.66)	0.62 (0.38)	0.83 (2.61)	158.78 (98.87)	1.20 (1.36)	2.43 (2.77)	0.25 (0.30)	1.07 (1.35)	0.20 (0.21)	2.20 (5.70)	0.20 (0.24)	0.51 (0.36)	4.54 (2.44)
PC	1.99 (1.24)	16.26 (14.33)	0.15 (0.10)	0.84 (0.66)	0.39 (0.47)	0.10 (0.07)	8.09 (5.74)	0.27 (0.24)	0.57 (0.42)	0.06 (0.04)	0.22 (0.16)	0.04 (0.03)	2.53 (6.64)	0.11 (0.08)	0.13 (0.07)	113.84 (32.64)
VSSM	0.33 (0.13)	3.86 (9.65)	0.03 (0.05)	0.22 (0.16)	0.08 (0.04)	0.04 (0.03	6.98 (4.82)	0.05 (0.06)	0.11 (0.13)	0.03 (0.03)	0.06 (0.06)	0.03 (0.02)	3.11 (5.73)	0.31 (0.37)	0.03 (0.02)	11.44 (11.34)
ZURI	1.20 (1.32)	24.20 (28.59)	0.12 (0.10)	1.06 (0.83)	0.30 (0.19)	0.03 (0.14)	15.72 (8.79)	0.19 (0.17)	0.41 (0.05)	0.10 (0.09)	0.15 (0.12)	0.06 (0.05)	2.40 (3.86)	0.64 (0.49)	0.10 (0.08)	3.76 (4.31)

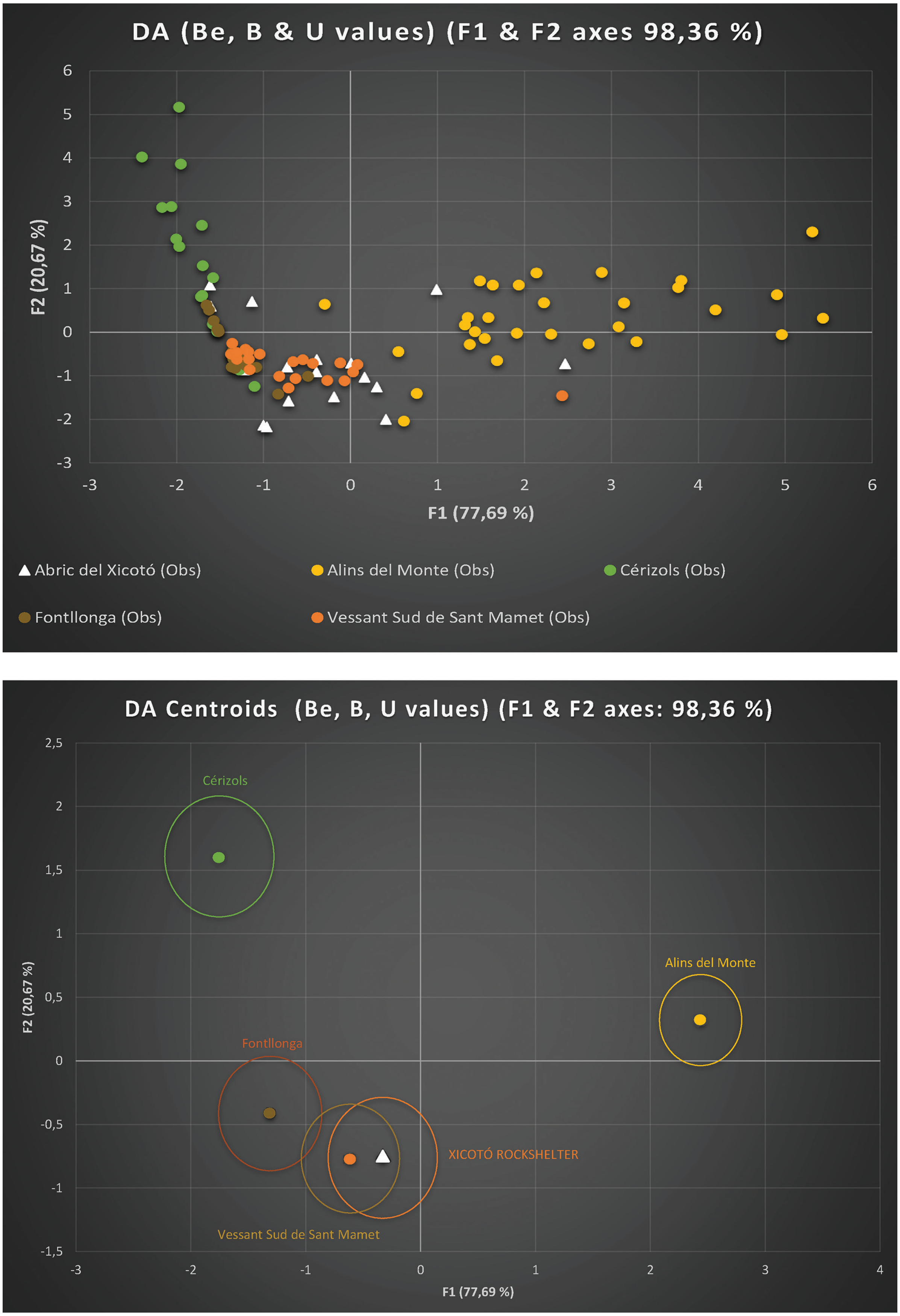

Figure 6. Results of Discriminant Analysis (DA) of the Be, B and values representing the evaporithic geological outcrops (circles) and the evaporithic archaeological samples of Xicotó (triangle) with all the samples (top) and just the centroids (bottom).

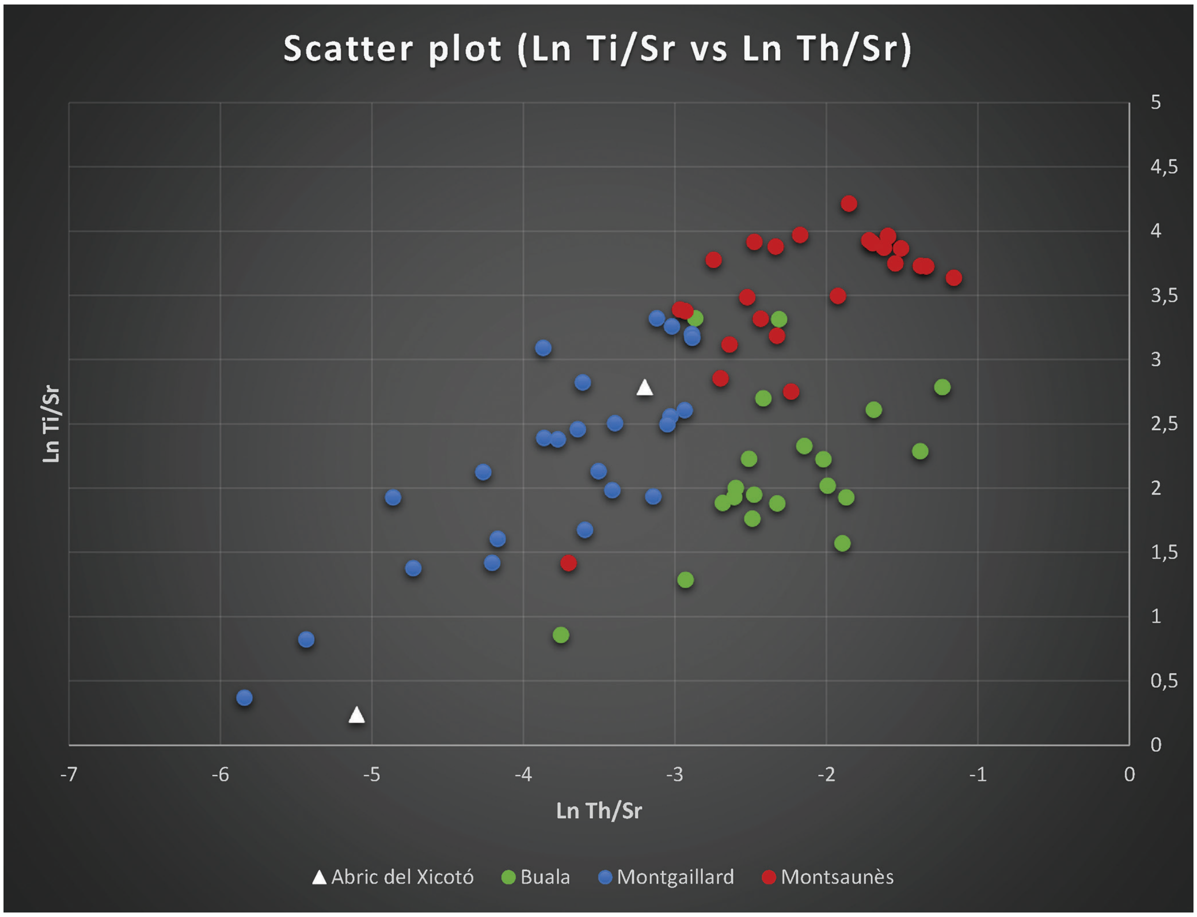

Figure 7. Scatterplot for Ln Ti/Sr vs Ln Th/Sr representing all the marine geological outcrops (circles) and the marine archaeological samples of Xicotó (triangle).

Garumnian facies of the Tremp Formation, outcropping in the Pre-Pyrenean ranges. Moreover, the geochemical analysis has established significant differences between outcrops, which has thus allowed the studied archaeological artefacts to be connected with samples from the Vessant Sud de Sant Mamet outcrop. This is the closest outcrop to the site, being located less than 5 km to the north of Xicotó. Probably because this chert type has a smooth grain and its capability for knapping is not extraordinary, human groups from the Middle Mesolithic also frequented the chert outcrops from Castelló de Farfanya, in the Serra Llarga Mountain Range, according to the geochemical study. These outcrops are located at 25–30 km to the south-east of Xicotó and have fine grains and high-knapping capabilities, being the better-quality chert outcrops nearest to the site. Moreover, the presence of two marine cherts in the Middle Mesolithic occupation that seem to fit with the Montgaillard chert outcrop, at more than 100 km distance in the northern central Pyrenees, could indicate the existence of contacts with northern groups. However, we need to be particularly cautious with these results, as they are only two pieces of evidence in an almost local lithic assemblage and other possible explanations could be considered.

Taking into account that the geochemical analysis of chert has only been developed with artefacts recovered from the Middle Mesolithic unit, in further work we will try to relate these results with other Middle Mesolithic sites from the Pyrenean and Pre-Pyrenean region. The Notches and Denticulates Mesolithic (also known as the Macrolithic Mesolithic) has been attested in the southern Pre-Pyrenean region, with similar procurement strategies as that observed in Xicotó Rockshelter. Thus, in the level Ib of Forcas II Rockshelter (Graus, Huesca), the Macrolithic Mesolithic is represented by some lithic samples of local origin (Utrilla and Mazo, 2014) and in the Peña 14 and Legunova (Biel, Zaragoza) assemblages, the local cherts are heavily exploited (García-Simón, 2018). Similarly, in the Western Pyrenean site of Atxoste (Mendandia, Álava), the local cherts are also predominant, the presence of more exogenous varieties being largely anecdotal (Soto *et al.*, 2015). In the south-eastern Pyrenees, the open air sites of Font del Ros (Berga, Barcelona) and Sota Palou (Campdevànol, Girona) have also revealed the main use of local materials for confectioning the lithic assemblage (Terradas, 1995). A similar strategy was also observed in the Mesolithic occupation of Balma del Guilanyà (Navès, Lleida) (Martínez-Moreno *et al.*, 2016) and the Pyrenean site of Balma Margineda (Aixovall, Andorra) (Guilaine *et al.*, 2008). We are faced with groups that culturally break with the previous lithic traditions, regarding the technology, the typology and the provenance of the

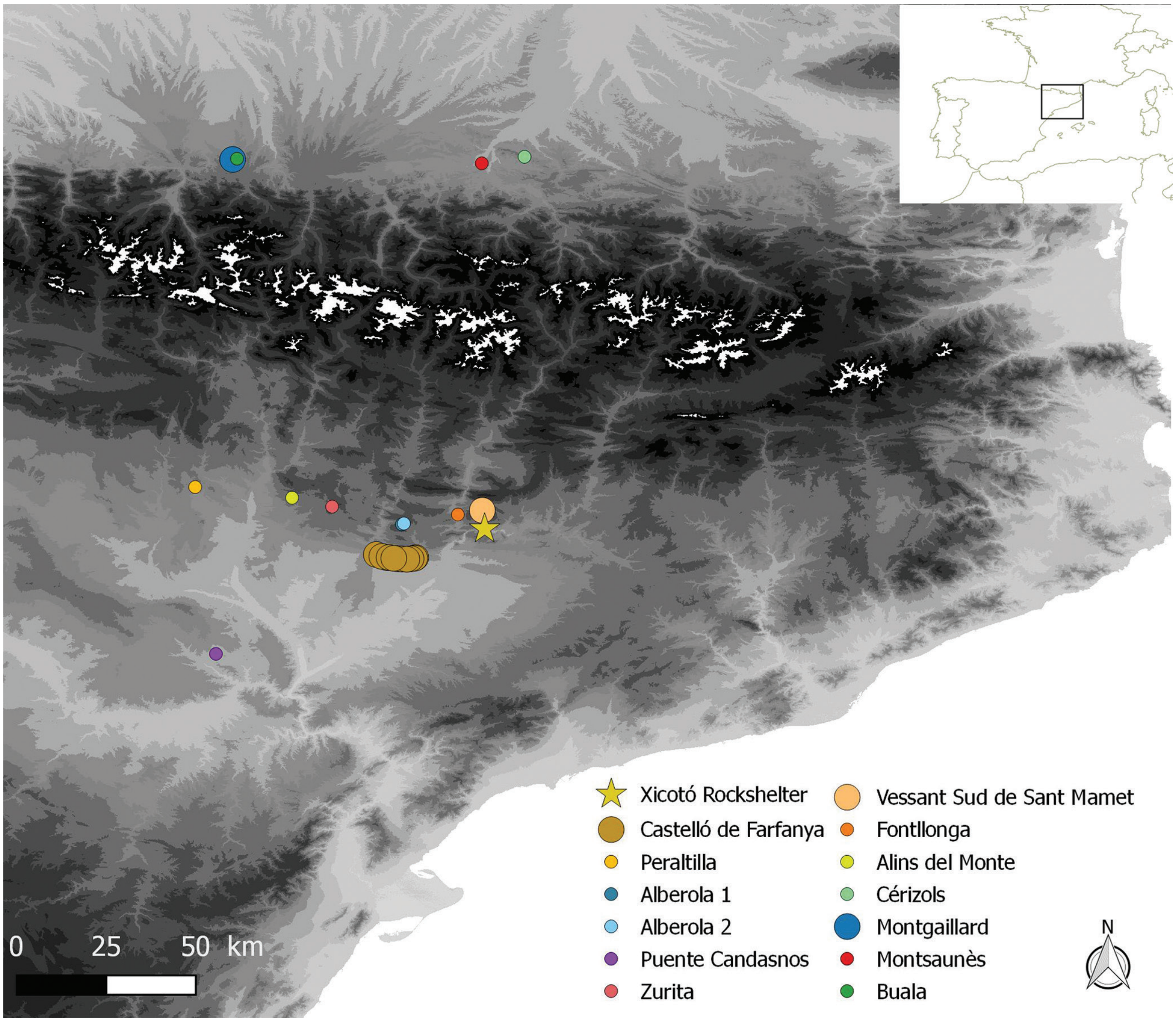

Figure 8. Location of the archaeological site of Xicotó and the different chert outcrops considered in the study. The largest circles correspond to the frequented outcrops according to the geochemical data.

lithic assemblage. During the Middle Mesolithic, it seems clear that the local cherts were almost always sufficient for confectioning lithic tools, regardless of the quality. Probably due to new climatic and environmental conditions, the use of wooden artefacts is strongly related to these changes. Following this assumption, human groups would be forced to adapt to the exploitation of this new environment, and the changes in their lithic acquisition strategies would most likely be a reflection of these adaptations.

5. Conclusions

In this paper we have presented the archaeological sequence revealed until now at Xicotó Rockshelter, as well as the results of our analysis of the lithic raw materials. The archaeological investigation has demonstrated that the site, at the very least, was frequented by prehistoric human groups during the Ancient Neolithic and the Notches and Denticulates Middle Mesolithic periods. The nature of the lithological assemblage has revealed that different activities took place in each period. The study of the chert artefacts, however, has presented similar results for both periods, with a main source of the local cherts being from the Vessant Sud de Sant Mamet outcrop and a regular source being from the Serra Llarga Mountain Range (Castelló de Farfanya outcrop). The presence of only two long-distance chert specimens in the Mesolithic period could indicate that eventual contacts with other groups may have existed. Forthcoming archaeological research will help us to better understand this Mesolithic occupation, as well as define the existence of previous human occupations at the site.

Acknowledgements

The research leading to these results has received funding from the postdoctoral fellowship program Beatriu de Pinós, funded by the Secretary of Universities and Research (AGAUR) (Government of Catalonia) and by the Horizon 2020 program of research and innovation of the European Union under the Marie Skodowska – Curie grant agreement No. 801370, held by M. Sánchez de la Torre. Archaeological works have been supported by the University of Barcelona and the project CLT009/18/00030 from the Catalan Government. This study was also financially supported by the Spanish project by the Spanish project PID2020-113960GB-I00, the French National Research Agency (ANR) (Grant No. ANR-10-LABX-52) and the project "The chronology of the Prehistory in NE Iberia" from the PALARQ foundation.

References

ADDINSOFT, 2020. *XLSTAT statistical and data analysis solution* [online]. New York, USA. [viewed 08/08/2022]. Available from: https://www.xlstat.com/

ALDAY, A.C., 2006. *El Mesolítico de muescas y denticulados en la cuenca del Ebro y el litoral mediterráneo peninsular.* Vitoria: Diputación Foral de Álava.

AUBRY, T., 1990. Problèmes de convergences de faciès siliceus: Exemple de l'approvisionnement en matières premières siliceuses des gisements solutréens et badegouliens du Centre de la France. In: M.R. Séronie-Vivien, and M. Lenoir, eds. *Le silex de sa genèse à l'outil.* Bordeaux: Cahiers du Quaternaire, pp. 433–442.

BARRAGUÉ, J., BARRAGUÉ, E., JARRY, M., FOUCHER, P., and SIMONNET, R., 2001. Le silex du flysch de Montgaillard et son exploitation sur les ateliers du Paléolithique supérieur à Hibarette (Hautes-Pyrénées). *Paleo,* 13**,** 1–28.

BERGADÀ, M.-M., FULLOLA, J. M., and SERRAT, D., 2007. *Memòria de la prospecció geoarqueològica al curs mitjà del Segre.* Barcelona: Generalitat de Catalunya, Direcció General del Patrimoni Cultural.

GARCÍA-SIMÓN, L.M., 2018. *Sílex y territorio en la Cuenca del Ebro: los sílex Monegros y Evaporítico del Ebro vs las variedades locales durante la Prehistoria.* Unpublished thesis (PhD), Universidad de Zaragoza.

GRATUZE, B., 1999. Obsidian Characterization by Laser Ablation ICP-MS and its Application to Prehistoric Trade in the Mediterranean and the Near East: Sources and Distribution of Obsidian within the Aegean and Anatolia. *Journal of Archaeological Science,* 26**,** 869–881.

GRATUZE, B., 2014. Application de la spectrométrie de masse à plasma avec prélèvement par ablation laser (LA-ICP-MS) à l'étude des recettes de fabrication et de la circulation des verres anciens. In: P. Dillmann, and L. Bellot-Gurlet, eds. *Circulation des matériaux et des objets dans les sociétés anciennes.* Paris: Éditions Archives Contemporaines, pp. 243–272.

GUILAINE, J., BARBAZA, M., and MARTZLUFF, M., 2008. *Les excavacions a la Balma Margineda (1979–1991).* Andorra la Vella: Govern d´Andorra.

IGME, 1998. *1:50.000, Balaguer (hoja 359)*. Madrid: Instituto Geológico y Minero de España.

IGME, 2006. *Mapa Geológico de España 1:50.000, Os de Balaguer (hoja 327)*. Madrid: Instituto Geológico y Minero de España.

IGME, e.p. *1:50.000, Monzón (hoja 326)*. Madrid: Instituto Geológico y Minero de España.

IMAI, N., TERASHIMA, S., ITOH, S., and ANDO, A., 1996. 1996 compilation of analytical data on nine GSJ geochemical reference samples, "Sedimentary rock series". *Geostandards Newsletter,* 20**,** 165–216.

MANGADO, X., 2005. *La caracterización y el aprovisionamiento de los recursos abióticos en la Prehistoria de Cataluña: las materias primas silíceas del Paleolítico Superior Final y el Epipaleolítico.* BAR International Series, 1420. Oxford: Oxford University Press.

MANGADO, X., TEJERO, J.-M., FULLOLA, J.-M., PETIT, M.-À., and SÁNCHEZ DE LA TORRE, M., 2014. La Cova del parco (Alòs de Balaguer, La Noguera, Lleida). La secuencia magdaleniense. In: E. Carbonell, J.M. Bermúdez de Castro, and J.L. Arsuaga, eds. *Los cazadores recolectores del Pleistoceno y del Holoceno en Iberia y el estrecho de Gibraltar. Estado actual del conocimiento del registro arqueológico.* Burgos: Universidad de Burgos & Fundación Atapuerca, pp. 152–158.

MARTÍNEZ-MORENO, J., RODA, X., VEGA, S., PIZARRO, J., ROY-SUNYER, M., SAMPER, S., PLASENCIA, J., and MORA, R., 2016. Balma Guilanyà: el llegat dels caçadors-recol·lectors al Solsonès. *Oppidum,* 14**,** 24–35.

OMS, F.X., SÁNCHEZ DE LA TORRE, M., PETIT, M.-À., LÓPEZ-CACHERO, F. J., and MANGADO, X., 2019. Nuevos datos del VI y V milenio cal BC en el llano y Prepirineo de Lleida (NE de la Península Ibérica): el Abric del Xicotó y Les Auvelles. *MUNIBE Antropologia-Arkeologia,* 70**,** 93–107.

ORANGE, M., LE BOURDONNEC, F.-X., BELLOT-GURLET, L., LUGLIÈ, C., DUBERNET, S., BRESSY-LEANDRI, C., SCHEFFERS, A., and JOANNES-BOYAU, R., 2017. On sourcing obsidian assemblages from the Mediterranean area: analytical strategies for their exhaustive geochemical characterisation. *Journal of Archaeological Science: Reports,* 12**,** 834–844.

ORTEGA, D., 2002. Mobilitat i desplaçaments dels grups caçadors-recol·lectors a inicis del Paleolític superio a la regió pirinenca oriental. *Cypsela,* 14**,** 11–26.

RAMSEY, C.B., 2017. Methods for Summarizing Radiocarbon Datasets. *Radiocarbon,* 59**,** 1809–1833.

REIMER, P.J., BARD, E., BAYLISS, A., BECK, J.W., BLACKWELL, P.G., RAMSEY, C.B., BUCK, C.E., CHENG, H., EDWARDS, R.L., FRIEDRICH, M., GROOTES, P.M., GUILDERSON, T.P., HAFLIDASON, H., HAJDAS, I., HATTÉ, C., HEATON, T.J., HOFFMANN, D.L., HOGG, A.G., HUGHEN, K.A., KAISER, K.F., KROMER, B., MANNING, S.W., NIU, M., REIMER, R.W., RICHARDS, D.A., SCOTT, E.M., SOUTHON, J.R., STAFF, R.A., TURNEY, C.S.M., VAN DER PLICHT, J. 2013. IntCal13 and Marine13 Radiocarbon Age Calibration Curves 0–50,000 Years cal BP. *Radiocarbon,* 55**,** 1869–1887.

ROY-SUNYER, M., TARRIÑO-VINAGRE, A., BENITO-CALVO, A., TORCAL, R.M., and MARTINEZ-MORENO, J., 2013. Flint procurement in the Eastern Prepyrenees during the Early Upper Paleolithic: the 497C archaeological level of Cova Gran (Santa Linya, Lleida). *Trabajos De Prehistoria,* 70, 7–27.

SÁEZ, A., 1987. *Estratigrafía y sedimentología de las formaciones lacustres del tránsito Eoceno-Oligoceno del NE de la Cuenca del Ebro.* Unpublished thesis (PhD), Universitat de Barcelona.

SÁNCHEZ DE LA TORRE, M., 2015. *Las sociedades cazadoras-recolectoras del Paleolítico superior final pirenaico: territorios económicos y sociales.* Barcelona: SERP. Universitat de Barcelona.

SÁNCHEZ DE LA TORRE, M., ANGYAL, A., KERTÉSZ, Z., DUBERNET, S., LE BOURDONNEC, F.-X., CSEDREKI, L., FURU, E., PAPP, E., SZOBOSZLAI, Z., and SZIKSZAI, Z., 2017a. Trace element mapping of two Pyrenean chert deposits (SW Europe) by PIXE. *Nuclear Instruments and Methods in Physics Research Section B: Beam Interactions with Materials and Atoms,* 400**,** 58–64.

SÁNCHEZ DE LA TORRE, M., ANGYAL, A., KERTÉSZ, Z., DUBERNET, S., LE BOURDONNEC, F.-X., PAPP, E., SZOBOSZLAI, Z., TÖRÖK, Z., CSEPREGI, Á., and SZIKSZAI, Z., 2019a. Micro-PIXE studies on prehistoric chert tools: elemental mapping to determine Palaeolithic lithic procurement. *Archaeological and Anthropological Sciences,* 11**,** 2375–2383.

SÁNCHEZ DE LA TORRE, M., LE BOURDONNEC, F.-X., DUBERNET, S., GRATUZE, B., MANGADO, X., and FULLOLA, J.M., 2017b. The geochemical characterization of two long distance chert tracers by ED-XRF and LA-ICP-MS. Implications for Magdalenian human mobility in the Pyrenees (SW Europe). *STAR: Science & Technology of Archaeological Research,* 3**,** 15–27.

SÁNCHEZ DE LA TORRE, M., LE BOURDONNEC, F.-X., and GRATUZE, B., 2019b. Reconsidering prehistoric chert catchment sources: new data from the Central Pyrenees (Western Europe). *Archaeological and Anthropological Sciences,* 11**,** 947–957.

SÁNCHEZ DE LA TORRE, M., LE BOURDONNEC, F.-X., GRATUZE, B., DOMINGO, R., GARCÍA-SIMÓN, L.M., MONTES, L., MAZO, C., and UTRILLA, P., 2017c. Applying ED-XRF and LA-ICP-MS to geochemically characterize chert. The case of the Central-Eastern Pre-Pyrenean lacustrine cherts and their presence in the Magdalenian of NE Iberia. *Journal of Archaeological Science: Reports,* 13**,** 88–98.

SIMONNET, R., 1999. De la Géologie à la Préhistoire: le silex des Prépyrénées. Résultats et réfléxions sur les perspectives et les limites de l'étude des matières premières lithiques. *Paleo,* 11**,** 78–88.

SOTO, A., TARRIÑO, A., and ALDAY, A., 2015. Evolution of procurement and managements strategies of lithic raw materials in the Mesolithic of Atxoste (Álava, Spain). *In:* N. BICHO, C. DETRY, T.D. PRICE, and E. CUNHA, eds. *Muge 150th:* **The 150th Anniversary of the discovery of Mesolithic Schellmiddens, volume 2**. Cambridge: Cambridge Scholars Publising, pp. 61–74.

SOTO, M., 2015. *Áreas y estrategias de aprovisionamiento lítico de los últimos cazadores-recolectores en las montañas de Prades (Tarragona).* Unpublished thesis (PhD), Universitat Rovira i Virgili.

TERRADAS, X., 1995. Las estrategias de gestión de los recursos líticos del Prepirineo catalán en el IX milenio BP: el asentamiento prehistórico de la Font del Ros. *Treballs d'Arqueologia*, 3, p. 206.

TERRADAS, X., 2001. La gestión de los recursos minerales en las sociedades cazadoras-recolectoras. *Treballs d'Etnoarqueologia,* 4**,** p. 186.

UTRILLA, P., and MAZO, C., 2014. *La Peña de las Forcas (Graus, Huesca). Un asentamiento estratégico en la confluencia del Ésera y el Isábena,* Zaragoza: Departamento de Ciencias de la Antigüedad, Universidad de Zaragoza.

WILSON, S.A., 1998. *Data compilation for USGS reference material GSP-2, Granodiorite, Silver Plume, Colorado. U.S.* [online] Geological Survey Open-File Report [viewed 08/08/2022]. Available from: https://emrlibrary.gov.yk.ca/ygs/open_files/2019/2019-1/Appendix%20C/C4_QAQC/GSP-2_StandardInformation_USGS.pdf